INTERNATIONAL JOURNAL OF CLIMATOLOGY
Int. J. Climatol. (2014)
Published online in Wiley Online Library
(wileyonlinelibrary.com) DOI: 10.1002/joc.4099

RMetS
Royal Meteorological Society

UV variability in an arid region of Northwest China from measurements and reconstructions

Lunche Wang,[a,b]* Wei Gong,[a,b]* Lan Feng[c,d] and Bo Hu[e]

[a] *State Key Laboratory of Information Engineering in Surveying, Mapping and Remote Sensing (LIESMARS), Wuhan University, Hubei province, China*

[b] *International Research Center of Satellite Remote Sensing and Atmospheric Monitoring, Wuhan University, China*

[c] *Institute of Arid Meteorology of CMA, Key Laboratory of Arid Climate Change and Reducing Disaster of Gansu Province, Key Open Laboratory of Arid Climate Change and Disaster Reduction of CMA, Lanzhou, China*

[d] *Northwest Regional Climate Center, Lanzhou, China*

[e] *State Key Laboratory of Atmospheric Boundary Layer Physics and Atmospheric Chemistry (LAPC), Institute of Atmospheric Physics, Chinese Academy of Sciences, Beijing, China*

ABSTRACT: Ultraviolet radiation (UV) observed at Fukang (FK), China from 2004 to 2012 was used to investigate UV variability and its relationship with global solar radiation (G) under various sky conditions in Northwest China. Clearness index (K_t) was used for characterizing the sky conditions and UV model development, it was discovered that clear skies were the dominated sky conditions (48.72%), followed by partly cloudy (32.56%) and overcast (18.72%) skies. Daily F_{UV} (fraction of UV to G) increased from November to June with an annual mean of 4.00% at FK. Meanwhile, an efficient all-sky UV model under any sky conditions has been proposed by investigating the dependence of hourly UV irradiations on K_t and cosine of solar zenith angle μ. The model was assessed through the statistical indices: mean bias error (MBE), mean absolute bias error (MABE) and root mean square error (RMSE) whose values were 1.27 (−0.24), 4.64 (4.56) and 6.26% (6.14%), respectively at hourly (daily) basis. The model has also been tested at three other sites with distinctly different climates in China. Finally, daily UV radiation during 1961–2012 in Northwest China was reconstructed and annual mean daily UV irradiation was about 0.603 MJ m^{-2} d^{-1}. UV decreased at 0.62 KJ m^{-2} d^{-1}decade^{-1} during the whole study period and the decreases were sharpest in spring (3.28 KJ m^{-2} d^{-1}decade^{-1}), however, there was an increasing trend at the rate of 2.16 KJ m^{-2} d^{-1}year^{-1} since 1991.

KEY WORDS ultraviolet radiation; clearness index; reconstruction; long-term variability; Northwest China

Received 25 February 2014; Revised 24 May 2014; Accepted 6 June 2014

1. Introduction

Solar ultraviolet radiation (UV) reaching the Earth's surface is important for its role in the induction of various biological and chemical processes (Foyo-Moreno *et al.*, 2003; Gray *et al.*, 2010; Keppler *et al.*, 2012), which has received considerable attention over the past decades from scientific community and the general population for obtaining a better understanding of the interaction between the Earth's atmosphere and the solar radiant energy (Martinez-Lozano *et al.*, 1996; Trenberth *et al.*, 2009; Thomas *et al.*, 2012). Although comprising only a small fraction of the global solar radiation (G), UV radiation has the capacity to cause direct and immediate harm to virtually all living organisms (especially to human health), such as skin cancer and cataracts (Gallagher and Lee, 2006; Bilbao *et al.*, 2011). Ultraviolet radiation can weaken the human immune system and affect crop production and ocean bioproductivity (McKenzie *et al.*, 1999; Udo and Aro, 1999; Podstawczyńska, 2010). Therefore, a clear knowledge of UV level reaching the surface and its spatial and temporal availability is of great significance to a wide range of disciplines, such as agriculture production, global climate change, energy budget and human health (Satheesh and Moorthy, 2005; Zhao *et al.*, 2005; Gao *et al.*, 2010).

Accurate long-term UV measurements are difficult to obtain due to great difficulties in conducting accurate observations and proper quality control, which has led to the development of ground-based measurement networks programs (Junk *et al.*, 2007; Chubarova, 2008; Fitzka *et al.*, 2012). However, UV radiation observations are still too few in the world and their records are relatively short, the number of UV observations is very limited in China to date, particularly in the Northwest area (Hu *et al.*, 2007, 2010a; Wang *et al.*, 2013a). UV levels have to be estimated through radiative transfer models or satellite-based observations from a prescribed atmospheric state (Hu *et al.*, 2010b; Wang *et al.*, 2014b), for example, Mateos *et al.* (2010) developed several empirical models of hourly UV radiation in Valladolid, Spain; Herman (2010) estimated UV irradiance during 1979–2008 from satellite

* Correspondence to: L. Wang and W. Gong, State Key Laboratory of Information Engineering in Surveying, Mapping and Remote Sensing (LIESMARS), Wuhan University, Wuhan, Hubei 430079, China. E–mail: lunchewang@whu.edu.cn; liesmars_lidar@whu.edu.cn

data. Meanwhile, UV irradiation will be affected by cloud cover, total ozone column, surface albedo and atmospheric constituents, which make it difficult to estimate accurately the UV radiation under various sky conditions (Alados-Arboledas *et al.*, 2003; Cañada *et al.*, 2003; Esteve *et al.*, 2010); these models should be recalibrated to account for local geographical and atmospheric conditions (Kuchinke and Nunez, 1999; Escobedo *et al.*, 2009; Bano *et al.*, 2013). Therefore, it is still essential to have as many observations as possible on a continuous basis to make a detailed study of the variation characteristics of UV radiation (Calbó *et al.*, 2005; Josefsson, 2006; den Outer *et al.*, 2010).

Moreover, reconstruction of UV radiation during the last decades has gained scientific interest with respect to the well-known evolution of ozone layer and the general variation of climate (Fioletov *et al.*, 2001; Kvalevag *et al.*, 2009; Wang *et al.*, 2013b). Although Wei *et al.* (2006) have studied the long-term relationship between UV radiation and ozone in China using Total Ozone Mapping Spectrometer (TOMS) products, our earlier studies (Hu *et al.*, 2010a; Wang *et al.*, 2013a) have studied the interannual variations of UV radiation in Beijing and Wuhan during the past 50 years; Hu *et al.* (2010c) has preliminarily analysed the characteristics of UV radiation in arid and semi-arid regions of China, there is no more studies focusing on analysing the long-term trends of UV radiation in Northwest China, which make it necessary for developing efficient models for investigating UV variability in this area.

The main objective of this study is to analyse the hourly/daily variations of UV radiation and its relationship with G under different sky conditions in Northwest China using 8-year measurements. By investigating the relationship between UV radiation, cosine of solar zenith angle and clearness index (K_t), an efficient nonlinear statistical models for estimating hourly/daily UV radiation will be proposed, which will be tested at two other sites in China with different climate conditions. Hourly/daily UV radiation from 1961 to 2012 will be reconstructed; the possible reasons for the long-term trends will also be discussed.

2. Measurement sites and data analysis

2.1. Sites and instruments

The measurements used in this study were observed at Fukang (FK), Xinjiang Uygur Autonomous Region in Northwest China, which was affiliated to Chinese Ecosystem Research Network (CERN). CERN is the first standard network established to measure solar UV radiation for investigating the radiation budget and its spatial and temporal variation properties in China (Fu *et al.*, 2010). The station (44°17′N, 87°55′E and 460 m above sea level) named Fukang Desert Ecosystem Observation and Experiment Station was situated at the southern edge of Junggar Basin. FK station is broadly a representative of inland desert of temperate zone in the centre of Eurasia (Hu *et al.*, 2010c). As an area dominated by saline alkali arid soils, FK has a continental arid climate with a mean temperature of 6.6 °C; its annual mean precipitation is about 164 mm but the annual potential evaporation reaches 2000 mm (Hong *et al.*, 2008; Wang *et al.*, 2014a). Further climatological and meteorological details about the study area were given by Xu and Li (2006).

A series of solar radiation observation instruments have been installed at FK since August 2004. CM 11 pyranometer has been used for G (305–2800 nm) observation with an accuracy of 2–3%; UV radiation (290–400 nm) made by Kipp and Zonen, Delft, Netherland was measured by CUV3 with a relative error lower than 5%. All pyranometers were calibrated against reference pyranometers using the 'alternate method' (Hu *et al.*, 2007). The calibration process has been described clearly in Hu *et al.* (2007), which was conducted by the calibration centre of CERN. All radiation data was recorded at 1-min interval; hourly values were derived from the minute values through integrations. Routine maintenances have been done to ensure that the radiometers were positioned horizontally by monitoring and adjusting the levelling instruments attached to each of them (Hu *et al.*, 2010a; Wang *et al.*, 2013b). These details concerning these radiometers and methods of data acquisition have also been described in other studies (Howell *et al.*, 1983; Udo and Aro, 1999).

The radiation data at FK used in this study covered a period of about 8 years from September 2004 to December 2012. Hourly and daily measurements of UV and G from Sanya (SY, 18°13′N, 109°28′E and 3 m above sea level), Linze (LZ, 39°04′N, 99°35′E and 1375 m above sea level) and Lasha (LS, 29°40′N, 91°20′E and 3688 m above sea level) in China during 2009–2010 provided by CERN were also used here for evaluating the model performance. SY, LZ and LS were characterized by tropical marine monsoon climate, continental desert steppe climate and plateau temperate semi-arid monsoon climate, respectively. The detail information of above three sites can be found in our earlier study (Hu *et al.*, 2007).

2.2. Methodology and definitions

The radiometric ratio of UV to G (F_{UV}) was computed by summing the individual fluxes (UV and G) over the course of a day, then taking the ratio (F_{UV}) of the sums. The analysis has been limited to cases that solar elevation angle was higher than 5° (Hu *et al.*, 2010b) due to the cosine response problem in this article. As stated in our earlier study (Wang *et al.*, 2014b), quality control for G was mainly based on the criterion: G should be smaller than extraterrestrial global solar radiation G_0 in the same geographical location, G/G_0 should be larger than 0.03 and G also should be larger than the minimum values in continuous overcast conditions (Geiger *et al.*, 2002). Similarly, UV should be smaller than UV_0 at the top of atmosphere in the same geographical coordinates and UV/G must be in the range of 0.02–0.08, otherwise it was considered as questionable observation. The extraterrestrial G_0 can be expressed as:

$$G_0 = 24/\pi \times S_0 L_0 \times \left[(\pi/180)\,\gamma\,(\sin\delta\sin\varphi) + (\cos\delta\cos\varphi\sin\gamma)\right] \quad (1)$$

Table 1. Monthly mean values of UV(daily), G (daily) and F_{UV} (hourly and daily) at FK, China.

Month	UV ($MJ\,m^{-2}$)				G ($MJ\,m^{-2}$)					
	Mean	Max	Min	SD	Mean	Max	Min	SD	Hourly F_{UV}	Daily F_{UV}
January	0.22	0.40	0.06	0.07	5.79	10.15	1.39	2.14	4.03	3.80
February	0.40	0.76	0.13	0.12	9.38	17.39	2.82	6.95	4.31	4.26
March	0.62	1.01	0.16	0.15	15.76	23.62	3.38	4.09	3.98	3.93
April	0.79	1.11	0.18	0.20	20.24	28.15	3.26	5.65	3.97	3.90
May	0.98	1.31	0.28	0.23	23.73	32.20	5.91	6.28	4.15	4.13
June	1.07	1.33	0.22	0.22	25.43	33.00	3.63	6.08	4.20	4.20
July	1.00	1.31	0.20	0.23	23.83	30.94	3.34	6.25	4.20	4.19
August	0.88	1.20	0.15	0.21	21.55	28.74	2.64	5.73	4.15	4.08
September	0.69	0.98	0.14	0.16	17.72	24.10	2.28	4.37	3.96	3.89
October	0.45	0.69	0.08	0.12	12.24	19.09	1.06	3.67	3.75	3.68
November	0.24	0.41	0.06	0.08	6.85	12.21	0.94	2.97	3.70	3.50
December	0.16	0.38	0.05	0.06	4.43	9.43	0.85	2.02	4.08	3.61
Annual	0.62	1.33	0.05	0.35	15.49	33.00	0.84	7.59	4.02	4.00

Max: maximum; Min: minimum; SD: standard deviations; F_{UV} (%).

where S_0 is about $1367\,W\,m^{-2}$, L_0 represents correction factor of the Earth's orbit, δ is solar declination, γ is sunrise hour angle and φ is geographical latitude.

The clearness index K_t, which is the ratio of G to extraterrestrial irradiance on a horizontal surface and a good indicator for the absorption and scattering process of all atmospheric constituents (Udo, 2000; Cañada *et al.*, 2000; Esteve *et al.*, 2010) was used for classifying the sky conditions in Northwest China: overcast sky ($K_t < 0.35$), partly cloudy sky ($0.35 < K_t < 0.65$) and clear sky ($K_t > 0.65$) (Iqbal, 1983; Escobedo *et al.*, 2009; Wang *et al.*, 2013b). Then observations from 2004 to 2010 were used for model development and the remaining data for model validation. The model accuracy will be evaluated by the scatter plots of the linear relationship between measured and estimated values, the statistical estimators (in percentage): mean bias error (MBE), mean absolute bias error (MABE) and root mean square error (RMSE) will be illustrated for each model.

$$\begin{aligned}
\mathrm{MBE}\,(\%) &= \frac{100}{M_{\mathrm{ave}}}\left(\frac{\sum_{i=1}^{N}\left(E_i - M_i\right)}{N}\right)\\
\mathrm{MABE}\,(\%) &= \frac{100}{M_{\mathrm{ave}}}\left(\frac{\sum_{i=1}^{N}\left|E_i - M_i\right|}{N}\right)\\
\mathrm{RMSE}\,(\%) &= \frac{100}{M_{\mathrm{ave}}}\left(\frac{\sum_{i=1}^{N}\left(E_i - M_i\right)^2}{N}\right)^{0.5}
\end{aligned} \tag{2}$$

where E_i is the estimated value (ith number), M_i is the measured value, M_{ave} is the average of the measured values and N is the number of observations.

3. Results and discussion

3.1. UV variability and its relationship with G under different sky conditions

Table 1 showed monthly statistics of mean, maximum, minimum and standard deviations for daily G and UV irradiations. Both radiant fluxes generally reached higher values in summer, whereas lower values were observed in winter months. The monthly average daily total UV irradiations varied from $0.16\,MJ\,m^{-2}$ (in December) to $1.07\,MJ\,m^{-2}$ (in June) with annual mean value being about $0.62\,MJ\,m^{-2}$, correspondingly, the absolute maxima of the monthly average G was $25.43\,MJ\,m^{-2}$ in June and the minima $4.43\,MJ\,m^{-2}$ occurred in December. Above UV observations were generally higher than those (Table 2) in Beijing ($0.38\,MJ\,m^{-2}$), Luancheng ($0.43\,MJ\,m^{-2}$), Yucheng ($0.47\,MJ\,m^{-2}$), Fengqiu ($0.49\,MJ\,m^{-2}$), Wuhan ($0.49\,MJ\,m^{-2}$), Jiaozhouwan ($0.51\,MJ\,m^{-2}$), Changwu ($0.52\,MJ\,m^{-2}$), Sanjiang ($0.53\,MJ\,m^{-2}$) and Shapotou ($0.59\,MJ\,m^{-2}$), lower than those at Haibei ($0.67\,MJ\,m^{-2}$) and LS ($0.92\,MJ\,m^{-2}$) in China (Hu *et al.*, 2007, 2010a, 2010b, 2010c; Wang *et al.*, 2013a), which may be attributed to the different geographical locations and climate types, such as altitude, aerosol burden, water vapour and ozone concentrations. The findings can also be compared with those in other observations around the world, which were clearly shown in Table 2, for example, annual mean daily UV radiation was about 0.42, 0.55, 0.67, $0.83\,MJ\,m^{-2}$ in Łódź (Poland), Maceió (Brazil), New Delhi (India), Valencia (Spain), respectively (Cañada *et al.*, 2003; Murillo *et al.*, 2003; Jacovides *et al.*, 2006; Bano *et al.*, 2013). Similar comparisons have also been conducted in our earlier study (Wang *et al.*, 2014b), which will be further analysed in later studies.

It can be also seen from Table 1 that hourly F_{UV} (fraction of UV to G) generally increased from 3.70% in November to 4.20% in June; daily F_{UV} changed from 3.50% in November to 4.20% in June with annual mean value being 4.00% in the study area. $UV = \alpha \times G$ was further used for detecting the systematic relationships between UV and G at hourly and daily basis. Table 3 showed the monthly parameters of the linear regression results, it was clear that α changed from about 0.034 in November to 0.044 in June at hourly basis; α varied from 0.033 in November to 0.041 in June on daily basis. This seasonal distribution was consistent with that of water vapour content, which

Table 2. Annual mean daily UV and α (slope of linear regression between UV and G) at sites around the world.

Site	Environment	UV (MJ m^{-2})	α	References
FK, China	Rural	0.62	0.04 (hourly)	This study
			0.04 (daily)	This study
LS, China	Rural	0.92	0.046 (daily)	Hu *et al.*, 2007
Beijing, China	Rural	0.38	0.031 (daily)	Hu *et al.*, 2010a
LZ, China	Rural	0.66	0.038 (daily)	Hu *et al.*, 2010c
Aksu, China	Rural	0.61	0.041 (daily)	Hu *et al.*, 2010c
Shapotou, China	Rural	0.59	0.037 (daily)	Hu *et al.*, 2010c
Haibei, China	Rural	0.67	0.042 (daily)	Hu *et al.*, 2010b
Yucheng, China	Rural	0.47	0.037 (daily)	Hu *et al.*, 2007
Luanchen, China	Rural	0.43	0.035 (daily)	Hu *et al.*, 2010b
Changwu, China	Rural	0.52	0.04 (daily)	Hu *et al.*, 2010c
Wuhan, China	Urban	0.49	0.0401 (daily)	Wang *et al.*, 2013a
Fengqiu, China	Rural	0.49	0.04 (daily)	Hu *et al.*, 2010b
Sanjiang, China	Wetlands	0.53	0.042 (daily)	Hu *et al.*, 2007
Jiaozhouwan, China	Bay	0.51	0.042 (daily)	Hu *et al.*, 2007
Łódź, Poland	Urban	0.42	0.04 (daily)	Podstawczyńska, 2010
Maceió, Brazil	Urban	0.55	0.027 (daily)	Porfirio *et al.*, 2012
New Delhi, India	Urban	0.67	0.042 (daily)	Bano *et al.*, 2013
Valencia, Spain	Urban	0.83	0.05 (hourly)	Cañada *et al.*, 2003
Córdoba, Spain	Urban		0.042 (hourly)	Cañada *et al.*, 2003
Golden, Spain	Rural		0.045 (hourly)	Murillo *et al.*, 2003
Almeria, Spain	Coast		0.045 (daily)	Barbero *et al.*, 2006
Cairo, Egypt	Urban		0.035 (daily)	Robaa, 2004
Athalassa, Cyprus	island		0.033 (hourly)	Jacovides *et al.*, 2006
Pesqueira, Brazil	Urban		0.043 (daily)	Leal *et al.*, 2011
Araripina, Brazil	Urban		0.041 (daily)	Leal *et al.*, 2011
Kwangju, South Korea	Urban		0.077 (hourly)	Ogunjobi and Kim, 2004

Table 3. Parameters of the linear regression (UV $= \alpha \times G$) between UV and G.

Month	Hourly			Daily		
	α	R^2	N	α	R^2	N
January	0.0373 ± 0.0021^b	0.90	1447	0.0371 ± 0.0021^b	0.88	242
February	0.0417 ± 0.0019^b	0.95	1383	0.0406 ± 0.0020^b	0.87	215
March	0.0389 ± 0.0019^b	0.97	1967	0.0384 ± 0.0021^b	0.87	247
April	0.0387 ± 0.0018^b	0.99	2067	0.0384 ± 0.0021^b	0.95	231
May	0.0408 ± 0.002^b	0.99	2345	0.0404 ± 0.0022^b	0.97	242
June	0.0418 ± 0.0021^b	0.99	2254	0.0414 ± 0.0025^b	0.95	232
July	0.0415 ± 0.0022^b	0.99	2400	0.0413 ± 0.0024^b	0.97	217
August	0.0405 ± 0.0020^b	0.98	2299	0.0400 ± 0.0024^b	0.95	236
September	0.0388 ± 0.0021^b	0.99	2033	0.0382 ± 0.0023^b	0.96	270
October	0.0361 ± 0.0020^b	0.98	1776	0.0359 ± 0.0022^b	0.95	266
November	0.0335 ± 0.0022^b	0.92	1226	0.0330 ± 0.0024^b	0.90	242
December	0.0359 ± 0.0020^b	0.86	1178	0.0356 ± 0.0025^b	0.84	237
Annual	0.0401 ± 0.0019^b	0.98	22380	0.04 ± 0.0022^b	0.98	2877

R^2 is coefficient of determination (at confidence level of 95%), N is the sample number. b indicates standard error of estimate determined at the particular confidence level of 97%.

reached its maximum in summer for abundant rainfall and then began to decrease due to withdrawal of the monsoon. Water vapour generally absorbed the longwave radiation, leaving the UV spectral portion unchanged, so α increased from winter to summer months. Annual mean daily α was about 0.04 at FK, which was close to those in Changwu and Fengqiu in China, higher than those in Beijing (0.031), Luancheng (0.035), Yucheng (0.037) and LZ (0.038), lower than those in Aksu (0.041), Haibei (0.042) and LS (0.046) in China (Table 2) (Hu *et al.*, 2007; Hu *et al.*, 2010c; Hu *et al.*, 2010b). Daily α was also higher than those at Maceió (0.027) in Brazil and Cairo (0.035) in Egypt, lower than those at New Delhi (0.042) in India, Almeria (0.045) in Spain, Pesqueira (0.043) and Araripna (0.041) in Brazil. These differences in α may partly due to the scattering and absorption effects of aerosols, for example, most aerosol particles at FK in Northwest China mainly originated from the soil (mineral components), selective scattering by these fine particles caused a larger loss of UV than G (in proportion), which resulted in a lower α value in FK than that at Aksu and Haibei in China (Hu *et al.*, 2010c).

As stated in above section, K_t was a good indicator for characterizing sky conditions, so K_t was used to investigate

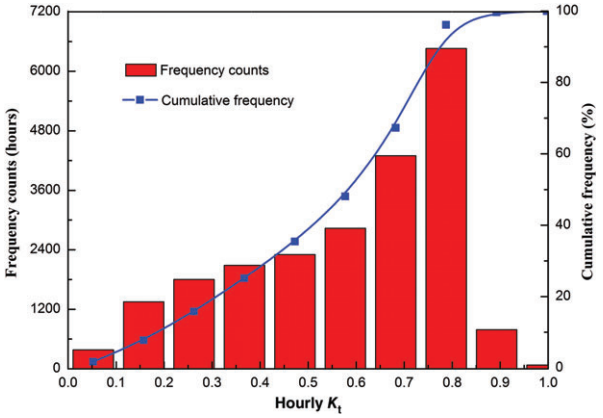

Figure 1. Frequency distributions of hourly K_t intervals during September 2004–December 2012.

the relationship between daily UV and G under various sky conditions for each month in Northwest China. Figure 1 showed the frequency distributions of hourly K_t intervals during the study period, it was obvious that clear skies were the dominated sky conditions (48.72%) at FK, followed by partly cloudy skies (32.56%) and overcast days (18.72%). Table 4 showed the linear regressions between daily UV and G under different sky conditions: under overcast skies, α increased from 4.24% in January to 4.89% in July (except in February), α then decreased gradually to the lower values in November (4.32%) and December (4.41%); for partly cloudy skies, α ranged from 3.50% in November to 4.33% in June; under clear skies, α increased from 3.24% in November to 4.10% in June at FK. At the same time, α decreased with K_t values for each month, for example, α in July changed from 4.89% under overcast conditions to 4.08% in clear skies. As was highlighted by de Miguel *et al.* (2011), the role played by the solar zenith angle on α is less determinant under overcast conditions. Similar findings have been reported in our earlier study (Wang *et al.*, 2014b), which may due to the fact that cloud effect is more influential for solar radiation in near-infrared spectrum than in UV band (Kylling *et al.*, 1997; Lopez *et al.*, 2009), although wavelengths below 320 nm suffer an enhanced ozone absorption under cloudy conditions (Mateos *et al.*, 2011).

3.2. UV model development and validation

3.2.1. UV estimation model

Several empirical/semi-empirical or physical models have been proposed for estimating UV radiation in literature, for example, UV irradiation can be estimated by considering its relationship with optical air mass and aerosol optical depth (Bano *et al.*, 2013). However, these models may not be suitable for other sites because they highly depended on the input variables, which indicated that these models should be recalibrated to account for local atmospheric and climate conditions (den Outer *et al.*, 2010; Wang *et al.*, 2013a). In this study, we introduced an efficient all-sky UV model for estimating UV radiation by investigating the dependence of hourly irradiation on K_t and cosine of solar zenith angle μ in Northwest China for the first time. A total of 70% of the radiation data at FK was used for model development and the remainders for validation. Figure 2 showed that hourly UV irradiations increased almost exponentially with μ for a giving specific K_t interval, this relationship was recommended to be described with power law equation (Xia *et al.*, 2008; Wang *et al.*, 2013a), which can be expressed by:

$$UV_h = UV_m \times \mu^b \tag{3}$$

where UV_m is the maximum UV irradiation per μ and b decides how UV irradiation changes with μ.

In order to simplify the complex nonlinear models, we divided the estimates of above model parameters in two steps. The relationship between UV_m and K_t was investigated by first binning K_t in 0.02 increments beginning at 0.03, power law equation was used to fit the data in each bin. UV_m for one unit μ then can be expressed as a cubic polynomial, that is to say, hourly maximum UV irradiation for one unit μ can be calculated. The regression analyses indicated that about 94% of hourly UV irradiation variability can be explained by Equation (3) and the

Table 4. Linear regression between daily UV and G for each month under different sky conditions.

	$K_t < 0.35$			$0.35 \le K_t < 0.65$			$K_t \ge 0.65$		
Month	α	R^2	N	α	R^2	N	α	R^2	N
January	0.0424	0.73	49	0.0386	0.72	127	0.0358	0.73	66
February	0.0487	0.87	21	0.0432	0.71	111	0.0403	0.87	88
March	0.0464	0.74	16	0.0401	0.56	84	0.0385	0.77	147
April	0.0465	0.90	21	0.0395	0.78	62	0.0384	0.82	148
May	0.0466	0.92	24	0.0420	0.89	83	0.0402	0.73	125
June	0.0475	0.90	19	0.0433	0.88	86	0.0410	0.32	127
July	0.0489	0.97	23	0.0423	0.88	91	0.0408	0.46	103
August	0.0485	0.92	22	0.0418	0.84	75	0.0400	0.70	139
September	0.0456	0.94	18	0.0402	0.90	70	0.0385	0.84	182
October	0.0448	0.85	23	0.0384	0.89	71	0.0355	0.90	172
November	0.0432	0.70	57	0.0350	0.58	84	0.0324	0.77	101
December	0.0441	0.72	72	0.0374	0.18	113	0.0335	0.40	52

R^2 is coefficient of determination and N is the sample number.

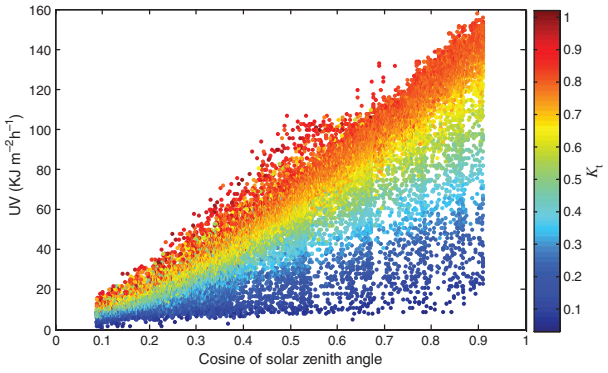

Figure 2. Dependence of hourly UV irradiations on K_t and cosine of solar zenith angle μ.

relative RMSE was about 4.6% at FK, statistical significances of the coefficients were also at 0.1% level given by the p values. Thus, the dependence of UV_m on K_t can be expressed as:

$$UV_m = -4.60 + 359.04K - 380.25K_t^2 + 239.01K_t^3 \quad (4)$$

The relationship between hourly UV irradiation and μ (through b) was further analysed. The values of b changed very little with standard deviation being 0.0015, p value of b was close to 0 and the statistical significance level was at 0.1%, so the estimate of 1.176 was obtained for b. Therefore, Equation (3) (in KJ m^{-2}) can be expressed as:

$$UV_h = \left(-4.60 + 359.04K_t - 380.25K_t^2 + 239.01K_t^3\right) \times \mu^{1.176} \quad (5)$$

Similarly, daily UV irradiation was also estimated by studying its dependence on daily mean K_t and cosine of solar zenith angle at noon. The p values of b were still close to 0 and the statistical significance levels of model parameters were still at 0.1%, the daily UV radiation (in MJ m^{-2}) can be obtained from:

$$UV_d = \left(0.03 + 2.57K_t - 1.35K_t^2 + 0.58K_t^3\right) \times \mu^{1.718} \quad (6)$$

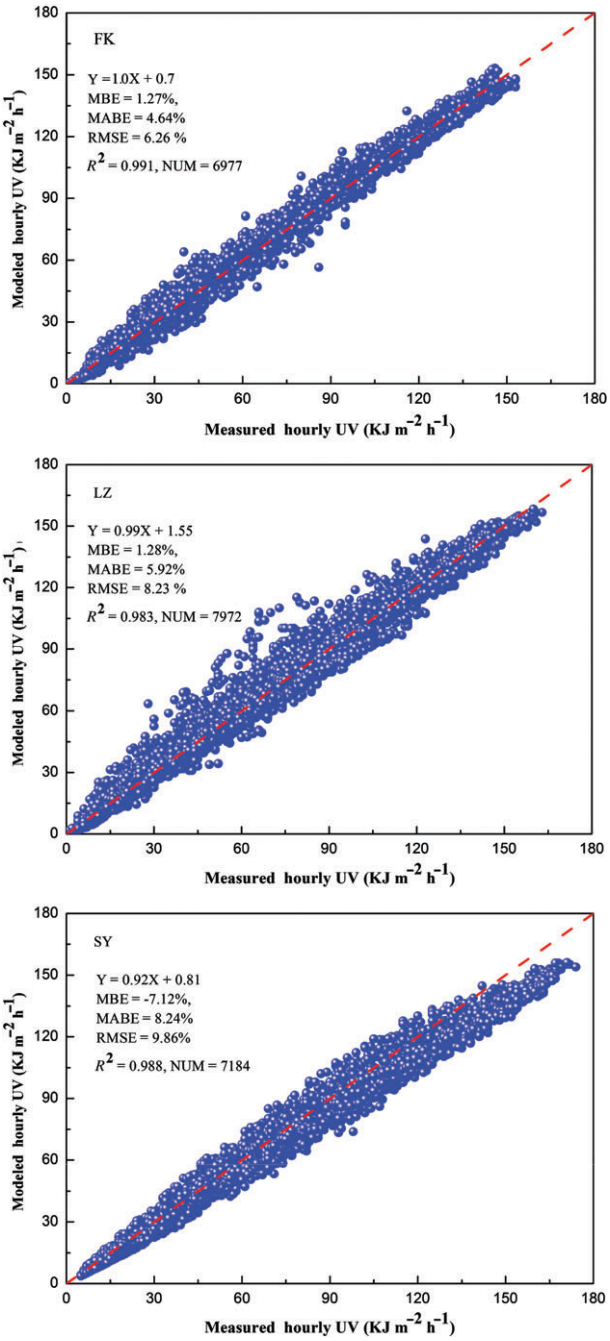

Figure 3. Scatterplot of hourly measured UV irradiation and estimates (dash line mean 1:1 relationship).

3.2.2. *Model validations*

Linear regression analysis between observed UV radiation and the estimates at FK were conducted to evaluate the model performance. As shown in Figure 3, 83% of the hourly estimates agreed well with the measurements to within 5% and the overall relative deviation was about 7.46%; MBE, MABE and RMSE were 1.27, 4.64 and 6.26%, respectively, which indicated that the model can produce satisfied hourly estimates at FK. Meanwhile, Equation (6) was also tested at two other sites (LZ and SY) in China, which was characterized by distinctly different climates described in the second section. MBE, MABE and RMSE were 1.28, 5.92 and 8.23%, respectively at LZ. As verification for SY, MBE, MABE and RMSE were −7.12, 8.24 and 9.86%, respectively; the relative difference was also less than 9.22%. Above statistical indices indicated that the all-sky UV model can also bring acceptable estimates in regions other than where the model was developed.

Moreover, regression analysis between daily UV estimates and measurements at FK indicated that the relative difference was also close to 6.76% (Figure 4); MBE, MABE and RMSE were −0.24, 4.56 and 6.14%, respectively. The statistical indices further revealed that MBE,

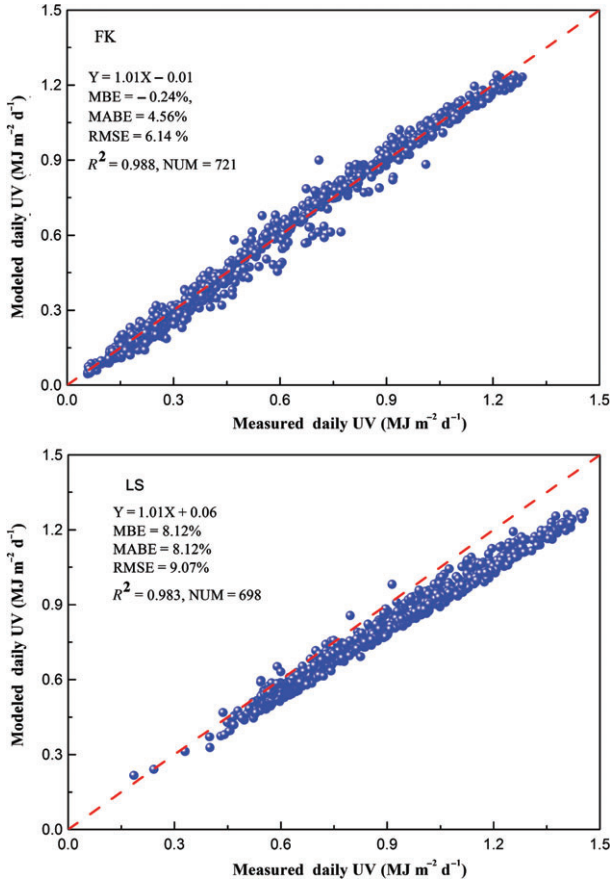

Figure 4. Scatterplot of daily measured UV irradiation and estimates (dash line mean 1:1 relationship).

MABE and RMSE were 8.12, 8.12 and 9.07%, respectively at LS; the relative deviation was about 8.76%. It can be seen from Figure 4(b) that modelled daily UV values at LS were generally higher than the measured values, so MBE and MABE have the same value in this condition. Although there were still some factors influencing the model performance, the analysis in this part showed that the model generally worked well under various sky conditions with high accuracy, which could be used for reconstructing UV radiation in Northwest China during the past decades.

3.3. Long-term variations of UV radiation in Northwest China

A series of algorithms for testing the *G* measurements have been applied in China to ensure the data quality (Shi *et al.*, 2008). Daily UV radiation at FK in Northwest China during 1961–2012 was reconstructed using above all-sky UV model based on *G* data set obtained from the National Meteorological Center. Annual and seasonal mean daily values were then obtained (winter was represented by December, January and February; spring was represented by March, April and May; summer was represented by June, July and August; autumn was represented by September, October and November). The 5-year moving average as well as linear regression analysis was used to analyse the temporal variations of annual and seasonal UV during 1961–2012. As shown in Figure 5 and Table 5, there was a decreasing trend for annual mean daily UV radiation at $-0.62\,\mathrm{KJ\,m^{-2}\,d^{-1}decade^{-1}}$ during 1961–2012 (statistically significant at the 95% confidence level), but UV radiation increased from the early 1990s at a rate of $2.16\,\mathrm{KJ\,m^{-2}\,d^{-1}year^{-1}}$; annual mean daily UV irradiation was about $0.603\,\mathrm{MJ\,m^{-2}\,d^{-1}}$ over the whole study period in Northwest China. This long-term variability may be consistent with that of daily *G*, which decreased steadily at about $44.33\,\mathrm{KJ\,m^{-2}\,d^{-1}year^{-1}}$ from 1961 to 1990 and then increased at a rate of $50.77\,\mathrm{KJ\,m^{-2}\,d^{-1}year^{-1}}$ for the year 1991–2012 (Table 5) ($-101.3\,\mathrm{KJ\,m^{-2}\,d^{-1}decade^{-1}}$ for the whole study period).

Meanwhile, *G* increased at the rate of 43, 79.59, 33.24 and $54.58\,\mathrm{KJ\,m^{-2}\,d^{-1}year^{-1}}$ in spring, summer, autumn and winter, respectively during 1991–2012. Table 5 and Figure 5 clearly showed the long-term variations of UV (and *G*) for each season, there were also decreasing trends of UV radiation in spring and winter months for the whole study period. The most significant decreasing was observed in spring at a rate of $-3.28\,\mathrm{KJ\,m^{-2}\,d^{-1}decade^{-1}}$ during 1961–2012. Long-term trend of UV radiation from 1961 to 2012 in summer and autumn were about 0.52 and $2.47\,\mathrm{KJ\,m^{-2}\,d^{-1}decade^{-1}}$, respectively. It was reported that annual mean daily UV radiation decreased at the rate of $18\,\mathrm{KJ\,m^{-2}\,d^{-1}decade^{-1}}$ in Beijing during 1958–2005, which was higher than that in Northwest China and may be due to the larger decreasing *G* in Beijing (Shi *et al.*, 2008; Hu *et al.*, 2010a). It was also discovered that UV radiation decreased at the rate of $5\,\mathrm{KJ\,m^{-2}\,d^{-1}year^{-1}}$ during 1961–1989 and then increased at $3\,\mathrm{KJ\,m^{-2}\,d^{-1}year^{-1}}$ for the period of 1990–2011 in Central China, which was generally consistent with the variation patterns in this study (Wang *et al.*, 2013a). Similar comparisons for more sites in China or other country will also be carried out later.

According to above descriptions, there was a decreasing trend for UV radiation in Northwest China from 1961 to 2012 and the decrease was sharper in spring, which may due to the combined effects of cloudiness, aerosol concentrations and water vapour (or local climates) (Wang and Shi, 2010). Much fossil fuel has been burned to achieve the rapid economic development in China, which has led to the increased anthropogenic aerosol loadings during the past several decades. It was known that aerosol particles can both scatter and absorb the solar radiation components in the atmosphere, causing decreases in the UV part, which may be one of the main reasons for the decreasing UV levels (Wang *et al.*, 2011). There were also some natural phenomena influencing the temporal variation of UV radiation at specific years, for example, large volcanic eruptions directly resulted in the decreases in the amount of surface UV levels. Since the 1990s, Chinese government started to take measures for improving the air quality, which may be a reason for the slight increase in UV radiation in recent years (Fang *et al.*, 2009; Wang *et al.*, 2013a). We know that there were still some factors influencing the

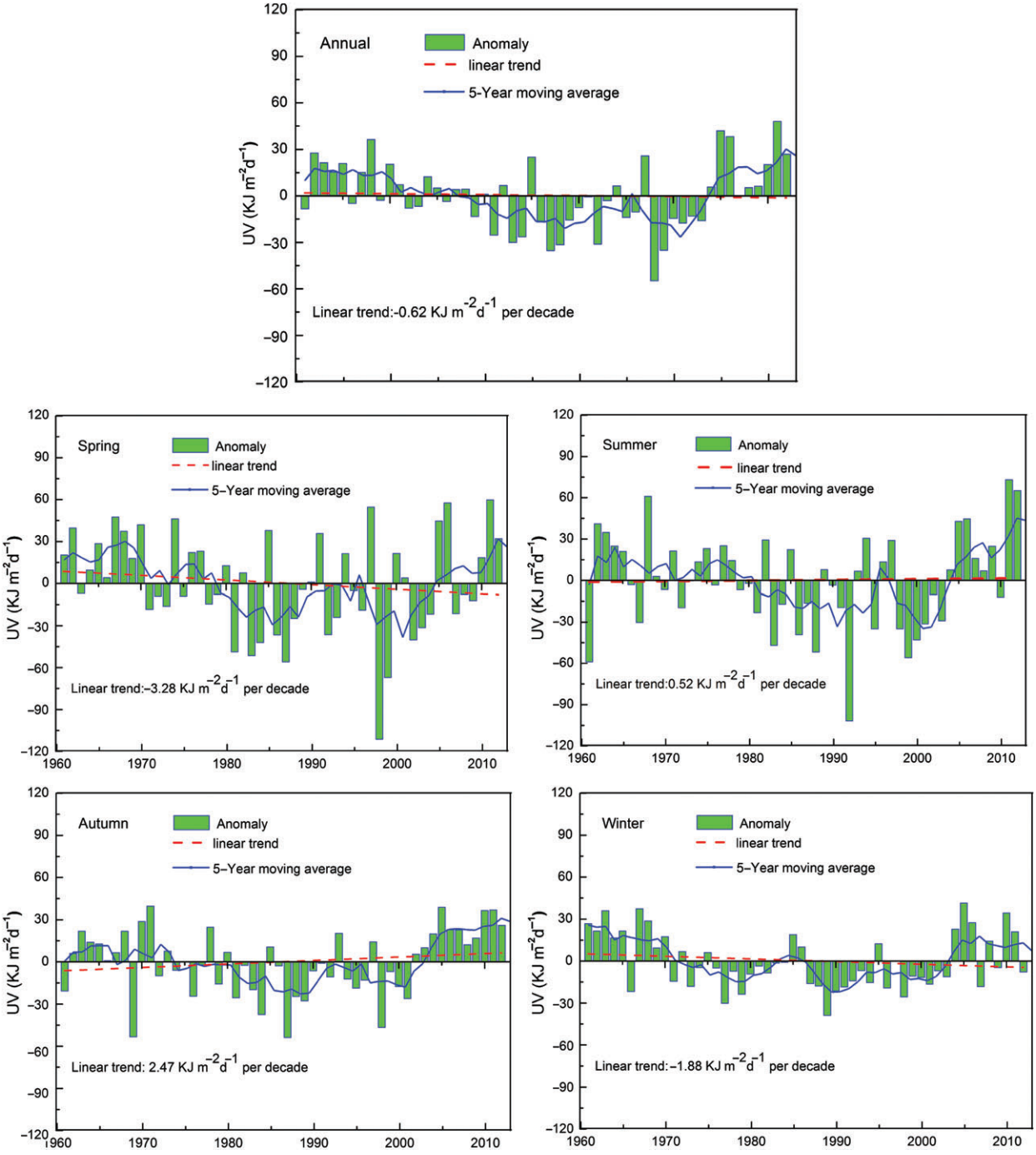

Figure 5. Interannual variations of annual and seasonal mean UV radiation in Northwest China.

long-term variations of UV radiation in Northwest China, which need to be further investigated in later studies.

4. Conclusion

Hourly and daily observations of UV and G at FK from September 2004 to December 2012 were used to investigate UV variability and its relationship with G under different sky conditions in Northwest China for the first time. Monthly average daily UV irradiations increased from 0.16 MJ m^{-2} in December to 1.07 MJ m^{-2} in June with annual mean value being 0.62 MJ m^{-2}. F_{UV} changed from 3.50% (3.70%) in November to 4.20% (4.20%) in June at daily (hourly) basis and the annual mean daily F_{UV} was about 4.00%. It was discovered that clear skies were the dominated sky conditions in Northwest China characterized by K_t, α also decreased with K_t values for each month, which may due to the fact that clouds/aerosols reduced G proportionally more than the UV part.

By analysing the dependences of UV irradiation on K_t and cosine of solar zenith angle μ, an efficient UV

Table 5. Linear trend of daily UV and G in Northwest China.

		1961–2012 ($KJ\,m^{-2}\,d^{-1}$ $decade^{-1}$)	1961–1990 ($KJ\,m^{-2}\,d^{-1}$ $year^{-1}$)	1991–2012 ($KJ\,m^{-2}\,d^{-1}$ $year^{-1}$)
UV trend	Annual	−0.62	−1.33	2.16
	Spring	−3.28	−1.81	1.72
	Summer	0.52	−0.99	2.03
	Autumn	2.47	−1.09	2.20
	Winter	−1.88	−1.41	1.52
G trend	Annual	−101.3	−43.33	50.77
	Spring	−168.16	−54.49	43
	Summer	−79.64	−32.36	79.59
	Autumn	−42.27	−34.45	33.24
	Winter	−113.9	−50.76	54.58

model under any sky condition at hourly/daily basis has been introduced and the statistical results showed that the model can produce satisfied estimates at FK: MBE, MABE and RMSE were only 1.27 (−0.24), 4.64 (4.56) and 6.26% (6.14%), respectively at hourly (daily) basis. The models were also validated at LZ, SY and LS in China. Daily UV irradiations from 1961 to 2012 were then reconstructed based on G observations and the annual mean daily UV value was about $0.603\,MJ\,m^{-2}\,d^{-1}$. It was discovered that there was a decreasing trend for UV radiation in Northwest China (at a rate of $0.62\,KJ\,m^{-2}\,d^{-1}decade^{-1}$) and the decreasing was sharpest in spring at $3.28\,KJ\,m^{-2}\,d^{-1}decade^{-1}$; the most significant increasing of UV radiation was observed at autumn ($2.47\,KJ\,m^{-2}\,d^{-1}decade^{-1}$) during 1961–2012. Annual mean UV radiation also increased since 1991 at the rate of $2.16\,KJ\,m^{-2}\,d^{-1}year^{-1}$, which may due to the reducing aerosol emissions in recent years.

The analysis in this article improves the basic understanding of UV variability and its relationship with G in Northwest China. The proposed model may be used for estimating UV radiation at national scale in China, which will play fundamental role in many fields such as ecological processes, atmospheric environment, energy budget and human health effects. There are still some factors influencing the model accuracy, which should be considered in our next work for improvement.

Acknowledgements

This work was financially supported by National Basic Research Program (grant no. 2011CB707106) and National Natural Science Foundation of China (NSFC) (Program: no. 41127901). We would like to thank the observation team of Chinese Ecosystem Research Network (CERN) for their hard work in collecting data. The global solar radiation data from 1961 to 2012 used in this study was obtained from the CMA/National Meteorological Centre, which was highly appreciated by the authors. We also express our sincere gratitude to all members of Lidar team in Liesmars, Wuhan University, China.

References

Alados-Arboledas L, Alados I, Foyo-Moreno I, Olmo FJ, Alcántara A. 2003. The influence of clouds on surface UV erythemal irradiance. *Atmos. Res.* **66**: 273–290.

Bano T, Singh S, Gupta NC, John T. 2013. Solar global ultraviolet and broadband global radiant fluxes and their relationships with aerosol optical depth at New Delhi. *Int. J. Climatol.* **33**: 1551–1562.

Barbero FJ, Lopez G, Batlles FJ. 2006. Determination of daily solar ultraviolet radiation using statistical models and artificial neural networks. *Ann. Geophys.* **24**: 2105–2114.

Bilbao J, Miguel D, Miguel A. 2011. Analysis and cloudiness influence on UV total irradiation. *Int. J. Climatol.* **31**: 451–460, DOI: 10.1002/joc.2072.

Calbó J, Pagès D, González JA. 2005. Empirical studies of cloud effects on UV radiation: a review. *Rev. Geophys.* **43**: RG2002, DOI: 10.1029/2004RG000155.

Cañada J, Pedrós G, López A, Boscá JV. 2000. Influences of the clearness index for the whole spectrum and of the relative optical air mass on UV solar irradiance for two locations in the Mediterranean area, Valencia and Cordoba. *J. Geophys. Res.* **105**: 59–4766.

Cañada J, Pedros G, Bosca JV. 2003. Relationships between UV (0.290–0.385 μm) and broad band solar radiation hourly values in Valencia and Cordoba, Spain. *Energy* **28**: 199–217.

Chubarova NY. 2008. UV variability in Moscow according to long-term UV measurements and reconstruction model. *Atmos. Chem. Phys.* **8**: 3025–3031.

Escobedo JF, Gomes EN, Oliveira AP, Soares J. 2009. Modeling hourly and daily fractions of UV, PAR and NIR to global solar radiation under various sky conditions at Botucatu, Brazil. *Appl. Energy* **86**: 299–309.

Esteve AR, Marín MJ, Tena F, Utrillas MP, Martinez-Lozano JA. 2010. Influence of cloudiness over the values of erythemal radiation in Valencia, Spain. *Int. J. Climatol.* **30**: 127–136.

Fang M, Chan CK, Yao XH. 2009. Managing air quality in a rapidly developing nation, China. *Atmos. Environ.* **43**: 79–86.

Fioletov VE, McArthur LJ, Kerr JB, Wardle I. 2001. Long-term variations of UV-B irradiance over Canada estimated from Brewer observations and derived from ozone and pyranometer measurements. *J. Geophys. Res.* **106**: 23009–230027.

Fitzka M, Simic S, Hadzimustafic J. 2012. Trends in spectral UV radiation from long-term measurements at Hoher Sonnblick, Austria. *Theor. Appl. Climatol.* **110**: 585–593.

Foyo-Moreno I, Alados I, Olmo FJ, Alados-Arboledas L. 2003. The influence of cloudiness on UV global irradiance (295–385 nm). *Agr. Forest. Meteorol.* **120**: 101–111.

Fu BJ, Li SG, Yu XB, Yang P. 2010. Chinese ecosystem research network: progress and perspectives. *Ecol. Complexity* **7**: 225–233.

Gallagher RP, Lee TK. 2006. Adverse effects of ultraviolet radiation: a brief review. *Prog. Biophys. Mol. Biol.* **92**: 119–131.

Gao W, Schmoldt DL, Slusser JR. 2010. *UV Radiation in Global Climate Change*. Tsinghua University Press: Beijing; Springer-Verlag: Berlin and Heidelberg, Germany, 2–17.

Geiger M, Diabate LM, Wald L. 2002. A web service for controlling the quality of measurements of global radiation. *Solar Energy* **73**: 475–480.

Gray LJ, Beer J, Geller M, Haigh JD, Lockwood M, Matthes K, Geel BV, White W. 2010. Solar influences on climate. *Rev. Geophys.* **48**: RG4001, DOI: 10.1029/2009RG000282.

Herman JR. 2010. Global increase in UV irradiance during the past 30 years (1979–2008) estimated from satellite data. *J. Geophys. Res.* **115**: D04203, DOI: 10.1029/2009JD012219.

Hong SK, Nakagoshi N, Fu BJ, Morimoto Y. 2008. *Landscape Ecological Applications in Man-Influenced Areas*. Springer: Dordrecht, The Netherlands, 87 pp.

Howell TA, Meek DW, Hatfield JL. 1983. Relationship of photosynthetically active radiation to shortwave radiation in the San Joaquin Valley. *Agr. Forest. Meteorol.* **28**: 157–175.

Hu B, Wang YS, Liu GR. 2007. Ultraviolet radiation spatio-temporal characteristics derived from the ground based measurements taken in China. *Atmos. Environ.* **41**: 5707–5718.

Hu B, Wang YS, Liu GR. 2010a. Variation characteristics of ultraviolet radiation derived from measurement and reconstruction in Beijing, China. *Tellus B* **62**: 100–108.

Hu B, Wang YS, Liu GR. 2010b. Properties of ultraviolet radiation and the relationship between ultraviolet radiation and aerosol optical depth in China. *Atmos. Res.* **98**: 297–308.

Hu B, Wang YS, Liu GR. 2010c. The characteristics of ultraviolet radiation in arid and semi-arid regions of China. *J. Atmos. Chem.* **67**: 141–155.

Iqbal M. 1983. *An Introduction to Solar Radiation*. Academic Press: New York, NY, 223.
Jacovides CP, Assimakopoulos VD, Tymvios FS, Theophilou K, Asimakopoulos DN. 2006. Solar global UV (280–380 nm) radiation and its relationship with solar global radiation measured on the island of Cyprus. *Energy* **31**: 2728–2738.
Josefsson W. 2006. UV-radiation 1983–2003 measured at Norrkoping, Sweden. *Theor. Appl. Climatol.* **83**: 59–76.
Junk J, Feister U, Helbig A. 2007. Reconstruction of daily solar UV irradiation from 1893 to 2002 in Potsdam, Germany. *Int. J. Biometeorol.* **51**: 505–512.
Keppler F, Vigano I, McLeod A, Ott U, Früchtl M, Röckmann T. 2012. Ultraviolet-radiation-induced methane emissions from meteorites and the Martian atmosphere. *Nature* **486**: 93–96.
Kuchinke C, Nunez M. 1999. Cloud transmission estimates of UVB erythemal irradiance. *Theor. Appl. Climatol.* **66**: 149–161.
Kvalevag MM, Myhre G, Myhre CEL. 2009. Extensive reduction of surface UV radiation since 1750 in world's populated regions. *Atmos. Chem. Phys.* **9**: 7737–7751.
Kylling A, Albold A, Seckmeyer G. 1997. Transmittance of a cloud is wavelength-dependent in the UV-range: physical interpretation. *Geophys. Res. Lett.* **24**: 397–400.
Leal SS, Tiba C, Piacentini R. 2011. Daily UV radiation modeling with the usage of statistical correlations and artificial neural networks. *Renew. Energy* **36**: 3337–3344.
Lopez ML, Palancar GG, Toselli BM. 2009. Effect of different types of clouds on surface UV-B and total solar irradiance at southern mid-latitudes: CMF determination at Cordoba, Argentina. *Atmos. Environ.* **43**: 3130–3136.
Martinez-Lozano JA, Tena F, Utrillas MP. 1996. Measurements and analysis of ultraviolet solar irradiation in Valencia, Spain. *Int. J. Climatol.* **16**: 947–955.
Mateos DM, Miguel A, Bilbao J. 2010. Empirical models of UV total radiation and cloud effect study. *Int. J. Climatol.* **30**: 1407–1415.
Mateos DM, di Sarra A, Meloni D, Di Biagio C, Sferlazzo DM. 2011. Experimental determination of cloud influence on the spectral UV radiation and implications for biological effects. *J. Atmos. Solar-Terrestrial Phys.* **73**: 1739–1746.
McKenzie R, Connor B, Bodeker G. 1999. Increased summertime UV radiation in New Zealand in response to ozone loss. *Science* **285**: 1709–1711.
de Miguel A, Mateos D, Bilbao J, Roman R. 2011. Sensitivity analysis of ratio between ultraviolet and total shortwave solar radiation to cloudiness, ozone, aerosols and perceptible water. *Atmos. Res.* **102**: 136–144.
Murillo W, Cañada J, Pedrós G. 2003. Correlation between global ultraviolet (290–385 nm) and global irradiation in Valencia and Cordoba (Spain). *Renew. Energy* **28**: 409–418.
Ogunjobi KO, Kim YJ. 2004. Ultraviolet (0.280–0.400 μm) and broadband solar hourly radiation at Kwangju, South Korea: analysis of their correlation with aerosol optical depth and clearness index. *Atmos. Res.* **71**: 193–214.
den Outer PN, Slaper H, Kaurola J, Lindfors A, Kazantzidis A, Bais AF, Feister U, Junk J, Janouch M, Josefsson W. 2010. Reconstructing of erythemal ultraviolet radiation levels in Europe for the past 4 decades. *J. Geophys. Res.* **115**: D10102, DOI: 10.1029/2009JD012827.
Podstawczyńska A. 2010. UV and global solar radiation in Łodź, Central Poland. *Int. J. Climatol.* **30**: 1–10.
Porfirio ACS, Souza JLD, Lyra GB, Lemes MAM. 2012. An assessment of the global UV solar radiation under various sky conditions in Maceió-Northeastern Brazil. *Energy* **44**: 584–592.
Robaa SM. 2004. A study of ultraviolet solar radiation at Cairo urban area, Egypt. *Solar Energy* **77**: 251–259.
Satheesh SK, Moorthy KK. 2005. Radiative effects of natural aerosols: a review. *Atmos. Environ.* **39**: 2089–2110.
Shi GY, Hayasaka T, Ohmura A, Chen HB, Wang B, Zhao JQ, Che HZ. 2008. Data quality assessment and the long-term trend of ground solar radiation in China. *J. Clim. Appl. Meteorol.* **47**: 1006–1016.
Thomas P, Swaminathan A, Lucas R. 2012. Climate change and health with an emphasis on interactions with ultraviolet radiation: a review. *Glob. Change Biol.* **18**: 2392–2405.
Trenberth KE, Fasullo JT, Kiehl J. 2009. Earth's global energy budget. *Bull. Am. Meteorol. Soc.* **90**: 311–323.
Udo S. 2000. Sky conditions at Ilorin as characterized by clearness index and relative sunshine. *Solar Energy* **69**: 45–53.
Udo SO, Aro TO. 1999. Global PAR related to global solar radiation for central Nigeria. *Agr. Forest. Meteorol.* **97**: 21–31.
Wang B, Shi GY. 2010. Long-term trends of atmospheric absorbing and scattering optical depths over China region estimated from the routine observation data of surface solar irradiances. *J. Geophys. Res.* **115**: D00K28, DOI: 10.1029/2009JD013239.
Wang CH, Zhang ZF, Tian WS. 2011. Factors affecting the surface radiation trends over China between 1960 and 2000. *Atmos. Environ.* **45**: 2379–2385.
Wang LC, Gong W, Ma YY, Hu B, Wang WL. 2013a. Analysis of ultraviolet radiation in Central China from observation and estimation. *Energy* **59**: 764–774.
Wang LC, Gong W, Lin AW, Hu B. 2013b. Measurements and cloudiness influence on UV radiation in Central China. *Int. J. Climatol.*, DOI: 10.1002/joc.3918.
Wang LC, Gong W, Hu B, Zhu ZM. 2014a. Analysis of photosynthetically active radiation in Northwest China from observation and estimation. *Int. J. Biometeorol.*, DOI: 10.1007/s00484-014-0835-3.
Wang LC, Gong W, Li J, Ma YY, Hu B. 2014b. Empirical studies of cloud effects on ultraviolet radiation in Central China. *Int. J. Climatol*. **34**: 2218–2228.
Wei K, Chen W, Huang RH. 2006. Long-term changes of the ultraviolet radiation in China and its relationship with total ozone and precipitation. *Adv. Atmos. Sci.* **23**: 700–710.
Xia X, Li Z, Crib M, Chen H, Zhao Y. 2008. Analysis of relationships between ultraviolet radiation (295–385 nm) and aerosols as well as shortwave radiation in North China plain. *Ann. Geophys.* **26**: 2043–2052.
Xu H, Li Y. 2006. Water-use strategy of three central Asian desert shrubs and their responses to rain pulse events. *Plant Soil* **285**: 5–17.
Zhao Y, Wang C, Wang S, Tibig LV. 2005. Impacts o f present and future climate variability on agriculture and forestry in the humid and sub-humid tropics. *Clim. Change* **70**: 73–116.

